Metal droplet entrainment by solid particles in slags: a combined phase field model and experimental approach

ir. Inge Bellemans[a], ir. Vincent Cnockaert[a], dr. Evelien De Wilde[a,b], prof. dr. ir. Nele Moelans[c], prof. dr. ir. Kim Verbeken[a]

[a] Ghent University, Department of Materials, textiles and chemical engineering
Technologiepark, 903
B-9052 Zwijnaarde (Ghent), Belgium

[b] Umicore Group Research & Development
Kasteelstraat 7
B-2250 Olen, Belgium

[c] KU Leuven, Department of Materials Engineering
Kasteelpark Arenberg 44, box 2450
B-3001 Heverlee (Leuven), Belgium

Keywords: Phase field model, Experiment, Metal droplet entrainment, Spinel, Slag

Abstract

Various pyrometallurgical industries (both primary and recycling) encounter production losses due to the mechanical entrainment of metallic droplets, i.e. the droplets are attached to solid particles in liquid slags. The attached metal cannot settle, decreasing the yield of the phase separation. This results in inadequate sedimentation and eventually production losses in e.g. industrial Cu smelters and Pb reduction melting furnaces.

Experimental work on this topic remains challenging, but phase field simulations can circumvent this lack of experimental data and allow a more systematic evaluation on the role of different parameters on the observed phenomenon. However, simulations are best interpreted in combination with experiments. The performed experiments are used both for the input microstructure of the solid particles and to validate the simulation results.

In the present work, a recently developed phase-field model to simulate the attachment of liquid metal droplets to solid particles in slags considering real microstructures of solid particles in liquid slags is extended to consider movement of the solid particles in the liquid slag. Furthermore, it is investigated which initialization method for the liquid metal droplets corresponds best to the experimental condi-

tions. One of the initialization methods used spinodal decomposition of a supersaturated slag to introduce the metallic droplets, whereas the other initialization consists of positioning metallic droplets in the slag in a random way. The simulations showed that both initialization methods result in microstructures that correspond with experimental observations, which points to the existence of several origins for the attachment of metal droplets to solid particles in slags.

1 Introduction

Metal extraction is based on the distribution of metals and impurities between two or more phases of which at least one contains a high concentration of the desired metal, for example by the reduction of Fe-rich ore, steel is made in a blast furnace. The distribution of the main metals and impurities between the phases is based on thermodynamic laws and therefore driven by composition, temperature, atmosphere, etc. Apart from the chemical distribution, the metals can only be recovered if a physical distribution also occurs. Here, a major issue is the entrainment of metal droplets in the oxide phase due to physical interactions between droplets and solid particles present in the liquid slag. This attachment creates production losses in industrial Cu smelters [1], Pb reduction melting furnaces [2] and other industries.

As mentioned above, these metal-oxide systems are influenced by composition, temperature, atmosphere, etc. To improve phase separations, the fundamental mechanisms governing the attachment of metal droplets to solid particles in liquid slags need to be identified which would require many experiments to investigate the influence of all parameters. Moreover, experimental investigation of this interaction remains very challenging. Consequently, available experimental results are scarce. However, the first experiments indicated that interfacial energies play an important role. The microstructure and composition of the phases can be investigated microscopically, but it is not straightforward to reveal the underlying chemical and physical phenomena as an experimental study of the effect of an individual parameter is very difficult, because it is almost impossible to keep the others constant.

Modelling can assist in gaining understanding of the evolution of microstructures and gives a more systematic insight into the role of some material properties. The physical and chemical properties of the system are well-controlled and the effect of each property can be investigated separately. The phase field method is a very powerful and versatile modelling technique for microstructural evolution. It was already used to model solidification [3, 4], solid-state phase transformations [5] and solid-state sintering [6].

In the phase field method, microstructures are represented by a set of field variables that are continuous functions of space and time. At interfaces, the field variables vary smoothly between the equilibrium values in the neighbouring grains. The position of the boundaries as a function of time is implicitly given by the field variables. This method avoids the mathematically difficult problems of applying boundary conditions at an interface whose position is part of the unknown solution. The phase field equations are derived from an energy functional according to thermodynamic principles. [7]

A previously developed phase field model [8, 9] describes the growth and evolution of liquid metal droplets by spinodal decomposition in a liquid oxide phase (representing the slag) with dispersed solid oxide particles in a model system. In our previously reported modelling work [8, 9], the influence of the interfacial energies on the attachment of metallic droplets to solid particles was investigated and four different wetting regimes were determined, namely no wettability of the metal on the particle, low wettability, high wettability and full wettability. [8] Moreover, the model was used to investigate the influence of the particle morphology on the behaviour of the liquid metal droplets in different wetting regimes. In addition, the simulations were used to classify and interpret experimental observations in a synthetic, but industrially relevant PbO-FeO-CaO-SiO_2-Cu_2O-ZnO-Al_2O_3 system [10], which corresponded best to the low-almost-no wetting regime.

In this study, the existing phase field model is extended to consider realistic microstructures based on actual micrographs of the slag with solid spinel particles which move at a certain speed in the liquid. Moreover, the origin of the attachment is investigated in more detail by comparing simulations using two different initialization methods for the metal droplets. First, the formulation of the model is presented, then the numerical implementation and simulation parameters are introduced. After which the results are presented and discussed and these are finally summarized at the end.

2 Model formulation

This work uses a phase field model to describe the droplet formation and growth in the presence of solid particles in a model system consisting of an oxide liquid (representing the slag) containing oxide particles and metallic droplets. The combination of a non-conserved phase-field variable ϕ and a conserved composition field x_M enables the description of the microstructural evolution of an isothermal hypothetical binary O-M (oxide-metal) system at constant pressure. ϕ is used to distinguish between the liquid phases ($\phi = 0$) and the solid particle ($\phi = 1$) and x_M represents the local molar fraction of the metallic element M. Both variables are position- and time-dependent and the position of the boundaries between the different phases is implicitly given by them, i.e. the variables continuously change from one bulk value to another bulk value over the interface. [7] It is assumed that the concentration of the solute in the precipitate is fixed and the molar volume V_m is the same in both phases and does not depend on composition.

2.1 Evolution equations

The microstructure evolution is driven by minimization of the total Gibbs energy. The evolution of the conserved variable is governed by the following mass balance equation

$$\frac{\partial x_M}{\partial t} = \nabla \left[M \nabla \left[\left(1 - h(\phi)\right) f'_{Liquid}(x_M) + h(\phi) f'_{Solid}(x_M) - \kappa_{x_M} \nabla^2 x_M \right] \right] \quad (1)$$

The coefficient M (m^5/ (J s)) is related to the interdiffusion coefficient D of the liquid as $D = A_{Sp} M \kappa_{XM}$ is the gradient energy coefficient for the liquid-liquid interfaces.

$$f_{Solid}(x_M) = \frac{A_S}{2}(x_M - x_S)^2$$

represents the bulk contribution of the solid phase. x_S and A_S (J/m³) are model parameters that determine the position of the minimum and the steepness of the parabola, describing the Gibbs energies as a function of the molar fraction of metal.

Analogously,

$$f_{Liquid}(x_M) = \frac{A_{Sp}}{2}(x_M - x_{eq,LO})^2(x_M - x_{eq,LM})^2$$

represents the homogeneous part of the free energy of the liquid phase. The corresponding free energy curve has a slope of A_{Sp} and two minima at $x_{eq,LO}$ and $x_{eq,LM}$. Where the oxidic liquid (slag) is indicated with 'LO', and the metallic liquid with 'LM'. The interpolation function $h(\phi)$ has the form

$$h(\phi) = \phi^3(10 - 15\phi + 6\phi^2)$$

.

With $h(\phi = 1) = 1$ in the solid and $h(\phi = 0) = 0$ in the liquid.

The non-conserved phase field variable ϕ evolves according to the following equation [11]

$$\frac{\partial \phi}{\partial t} = -L\frac{\delta F}{\delta \phi} = -L\left[W g'(\phi) + h'(\phi)\left(f_{Solid} - f_{Liquid}\right) - \kappa_\phi \nabla^2 \phi\right] \quad (2)$$

Where W is the depth of the double well function and $\kappa\phi$ the gradient energy coefficient for the solid-liquid interfaces.

In this study, rigid body motion of the solid particles with respect to the liquid is also included. For this, the Navier-Stokes equation for fluid flow will not be solved, which would correspond with the movement of the fluids with respect to the solid. In contrast, an equation is used to move the phase-field profiles in space, resulting in the displacement of the particle with respect to the liquids:

$$\frac{\partial \phi}{\partial t} = -\nabla \cdot \left[m_x h(\phi), m_y h(\phi)\right] \quad (3)$$

This equation represents the movement of the particle, where m_x and m_y determine the speed with which this happens. The equation is similar to the equations used in the level-set method [12, 13] and moves the ϕ-profile, after which the x_M adjusts itself to the new ϕ-profile. In theory, a convection equation should be established for x_M and the ϕ-value should adapt to this new x_M -value in the next time step. But in this study, a very small L-value was assumed (to simulate a non-reacting particle), which makes this second method very slow. To apply the rigid body motion equation, very small time steps are needed, for which a sub-cycling implementation was used.

2.2 Interface properties

Two types of interfaces are present: solid-liquid and liquid oxide-liquid metal. Both types are diffuse due to the gradient terms in the total energy expression. Following the approach of Cahn and Hilliard [14], the expression of the interfacial energy (J/m²) of the liquid-liquid interface $\gamma_{LO,LM}$ is:

$$\gamma_{LO,LM} = \frac{1}{6}\sqrt{\kappa_{x_M} A_{Sp}}\left(x_{eq,LM} - x_{eq,LO}\right)^3 \gamma_{L,L} = \frac{1}{6}\sqrt{\kappa_{x_M} A_{Sp}}\left(x_{eq,1} - x_{eq,0}\right)^3 \quad (4)$$

Especially noteworthy about this model is the expression for the solid-liquid interfacial energy (J/m²) $\gamma_{S,Lk}$ (with $k = O$ or M, when the oxide or the metal liquid is involved, respectively) as it consists of two contributions,

$$\gamma_{S,LO} \text{ or } \gamma_{S,LM} = \frac{1}{3\sqrt{2}}\sqrt{W\kappa_\phi} + \gamma_{S,Lk}^{\nabla x_M} \gamma_{S,L} = \frac{1}{3\sqrt{2}}\sqrt{W\kappa} + \gamma_{S,L}^{\nabla x_M} \quad (5)$$

The first term arises following the approach of Allen and Cahn [11] and the second term from the fact that a solid-liquid interface implies a change in both the phase field variable ϕ and the compositional variable x_M across the solid-liquid interface, yielding a non-zero gradient term for x_M. This contribution cannot be evaluated analytically. Thus, the following assumption was made: the composition dependence of the Gibbs energy across the interface is approximated by a spinodal function.

$$\frac{0.5\left(A_{Sp}+A_S\right)}{2}\left(x_M - x_S\right)^2\left(x_M - x_{eq,k}\right)^2 \quad (6)$$

This gives,

$$\gamma_{S,Lk}^{\nabla x_M} \approx \frac{1}{6}\sqrt{\kappa_{x_M} 0.5\left(A_{Sp} + A_S\right)}\left(\left|x_S - x_{eq,Lk}\right|\right)^3 \quad (7)$$

Constant parameters

In this study, a hypothetical O-M system is considered and as the model parameters can be linked with physical system properties, a typical order of magnitude was chosen for most parameters. The model parameters are listed in Table 1.

Table 1: Values and descriptions of several constant parameters in the model

Symbol	Description	Value(s)
N	System size	[256 256 1] grid points
Δx	Grid spacing	$(4/\sqrt{10})\ 10^{-7}$ m
Δt	Time steps spacing	10^{-4} s
$x_{eq,LO}$	Equilibrium compositions of free energy curve of spinodal	0.50
$x_{eq,LM}$	decomposition	0.98
A_{Sp}	Steepness of free energy curve of spinodal decomposition	$4\ 10^{8}$ J/m³
A_S	Steepness of free energy curve of solid	$20\ 10^{8}$ J/m³
W	Depth of the double well function	$15\ 10^{6}$ J/m³
$\kappa\phi$	Gradient energy coefficient for the solid-liquid interfaces	$(15/8)\ 10^{6}$ J/m
L	Kinetic coefficient for the evolution of ϕ	10^{-30} m³/(J s)
$L_{initial}$	Kinetic coefficient for the evolution of ϕ for the first 1000 time steps	10^{-7} m³/(J s)
κ_{xM}	Gradient energy coefficient for the liquid-liquid interfaces	$6\ 10^{-6}$ J/m
M	Mobility coefficient of the metal	10^{-19} m⁵/(J s)

According to literature [15, 16], $\gamma_{LO,LM}$ is of the order of 1 N/m. Furthermore, the interfaces should at least contain five grid points for a sufficient resolution of the diffuse transitions at interfaces and to reproduce accurately the surface energies [17]. With the values mentioned in Table 1, the liquid-liquid interfacial energy possesses the following constant value: $\gamma_{LO,LM}$ = 0.9030 N/m. And the interfacial widths possess the following values for all simulations: $l_{LO,LM}$ = 8.0687 grid points and $l_{S,LO}$ = 7.9057 grid points for the interface between solid and liquid oxide and $l_{S,LM}$ = 7.9057 grid points for the interface between solid and liquid metal. M is chosen such that the diffusion coefficient $D = 4\ 10^{-11}$ m²/s. It is assumed that the particle does not transform, providing a very small value of L.

2.4 Numerical implementation

A commercial software package Matlab 8.1 (R2013a) [18] was used for data processing. The semi-implicit Fourier spectral method [19] was employed to solve the kinetic equations numerically. Typical computation times on an Intel® Core™ i7-3610QM CPU @ 2.30GHz processor with 8 GB RAM ranged from 2 h to 4 h for a system size of [256 256 1] and a simulation time of 10^6 time steps. This simulation time of 10^6 time steps corresponds to 100 s.

2.5 Initialization

2.5.1 Real microstructure of a slag containing solid particles

Previous work [8, 9] only considered particles with simplified geometries. These simple morphologies approximate the spinel structure, which was observed for the solid particles to which the droplets attach in experiments. Previous simulations, however, also showed that the particle shape and distribution affect the amount of attached metal. Therefore, in this work the microstructure of the solid particles considered in the simulations was constructed based on actual experimental micrographs of these solid particles. In order to do this, the micrographs in the left hand side of Figure 1 were used as input for the 'imread' command in Matlab, turning every pixel of the photograph into a greyscale value. The micrographs are named photo 1 – 4 starting in the upper left corner to the lower right corner.

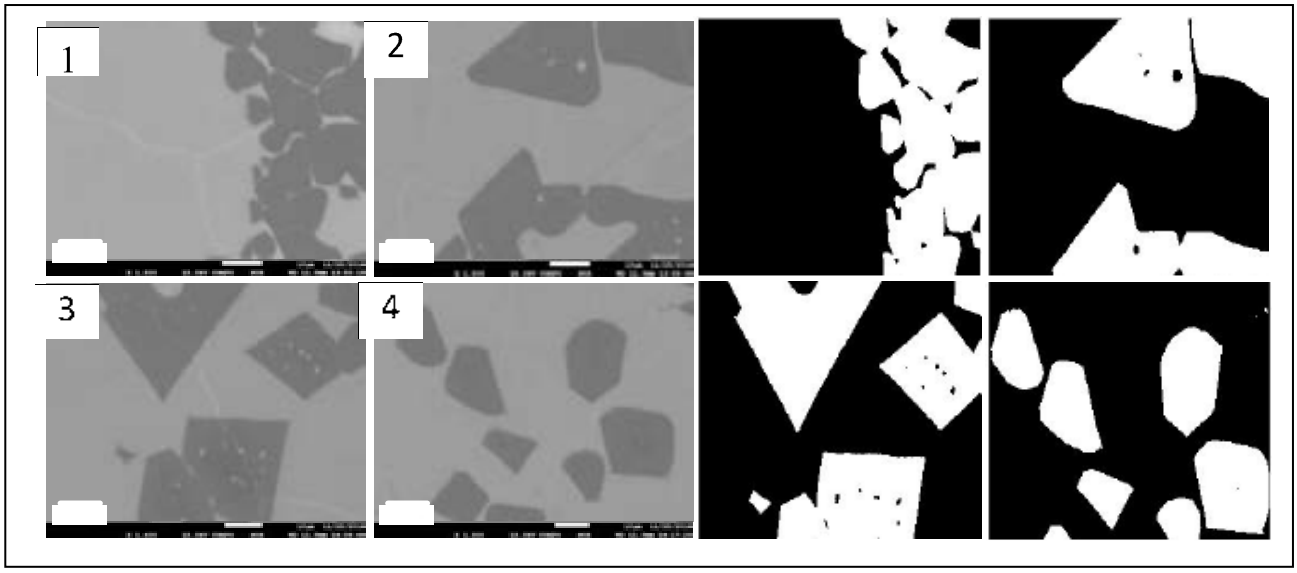

Figure 1: Left: SEM micrograph of experimentally obtained microstructure of solid oxide particles in a slag that was quenched to 'freeze' its high temperature condition [20];
Right: Black-and-white pictures that were used as initialization for the solid particles (white) within a liquid phase (black)

The edge with SEM information is then cut off, the pixels with a greyscale value above a certain threshold are treated as solid phase ($\phi = 1$) and the array containing these zeros and ones is then rescaled to the system size N in each dimension. The threshold value to which the greyscale values are compared is obtained by trial-and-error and can depend on the type of micrographs and the settings used to obtain them. For these SEM micrographs, a threshold value of 140 gave good results. This yielded the black-and-white figures in the right hand side of Figure 1, where white represents the solid ($\phi = 1$) and black the liquid ($\phi = 0$).

The corresponding particle fractions (defined by the area of all particles divided by the total system size, which is 65536 grid points for all cases) are tabulated in Table 2.

Table 2: The calculated particle fractions for every photograph

Photo	A = X*Y [grid points]	Particle density	P [grid points]	P/A [grid points^{-1}]
1	19964	0.305	1381	0.0692
2	23989	0.366	1255	0.0523
3	26868	0.410	1466	0.0546
4	18646	0.285	1280	0.0686

In reality, large variations are found (from 2 – 6 wt.-% [21] to 25 wt.-% [20]) in the particle fraction and the conditions of the slag production play a very important role in this value. These values, however, are averages over the complete slag phase and we are explicitly interested in regions with more solid particles. These regions were therefore considered in more detail in the experimentally obtained micrographs in Figure 1 and thus the simulations also deal with larger particle densities than the values averaged over the complete slag phase.

2.5.2 Comparison of two initialization methods for the metal droplets

The exact mechanism behind the interaction between the solid particles and liquid metal is not known. It is also not understood how and where the metal droplets originate. We compared two methods to initialize the metal droplets in the simulations: by spinodal decomposition of a supersaturated liquid (from now onward called 'spinodal initialization') and by a random positioning of droplets within the liquid phase (from now onward called 'random initialization'). The first would correspond in practice to a case where the droplets are formed by a reaction in which both the droplets and the spinel solids are involved. The latter corresponds to a situation where the droplets and particles are formed separately and independently and are then mixed in the slag. In both methods, the solid particles within the liquid slag are initialised by setting the value of ϕ equal to 1 and x_M equal to x_S within the areas corresponding to the solid particles in the original micrographs. The remaining liquid phase has a value of ϕ equal to 0.

The spinodal initialization provides an easy way to introduce the metals in the system. For decomposition into a liquid metal ($x_M = x_{eq,LM} = 0.98$) and a liquid oxide ($x_M = x_{eq,LO} = 0.50$), the uniform initial saturation of the solution x_i should be chosen between the inflection points of the spinodal liquid curve (where $\frac{\partial^2 G}{\partial x_M^2} < 0$) [22], namely: $0.601 < x_i < 0.879$. To initiate the spinodal decomposition, random noise is added, from a normal distribution with mean 0 and standard deviation 0.001, in every 100th time step. Industrial metal fractions in slags after sedimentation are of the order of 5 %. According to the lever rule, the minimal achievable value of the metal fraction in this model system is 0.211. Therefore, the x_i-values were kept minimal, but within the spinodal region. Furthermore, for $x_i > 0.66$, metal strands are formed instead of droplets in the model system. Therefore, an x_i value of 0.605 was chosen for the simulations, which corresponds to a volume fraction of metal of 0.219.

The alternative initialization method with 'random initialization' consists of randomly positioning droplets with a radius chosen from a discrete uniform random distribution between 1 and 10 times Δx

in the system until the proposed volume fraction of metallic droplets is reached or slightly exceeded. Before the droplets are finally positioned within the system, it is checked that no overlap is present with the solid phase or other droplets already present in the system. Whenever this is the case, another position is looked for within the system. If no appropriate position is found after 20 trials, the initialization is aborted and the simulation is started with the droplets positioned in the system until then. The droplets are immediately initialized with their equilibrium composition of 0.98 ($x_{eq,LM}$) and the slag in between the droplets is initialised with a composition of 0.50 ($x_{eq,LO}$). The volume fraction of metal droplets was 0.20, corresponding to x_i-values of 0.596, which is close to the value of xi used for spinodal decomposition, thus enabling us to compare both methods. The random noise term is not included in the simulations with random initialization.

2.6 Post-processing

A metal droplet is defined as the connected domain where $x_M - \phi x_S$ is larger than 0.71 and the particle where $0.5 < \phi$. To investigate the attachment of the droplets to the solid particle, quantitatively, the droplet was enlarged with 2 grid point layers around the droplet and the particle with 3 grid point layers. When these extended domains overlap, the droplets are considered to be 'attached'. The fraction of attached metal is defined as the ratio of the total area of the attached droplets to the total area of metal droplets in the system.

The microstructural evolution is illustrated by greyscale plots of $x_M - \phi\ x_S$, which are scaled to the interval [0 1] in such a way that values lower / higher than the minimum / maximum value are converted to the minimum/maximum, respectively. Thus, the particle appears as a black rectangle, the equilibrium metallic phase as white, the equilibrium oxidic phase as grey.

3 Results and Discussion

The influence of rigid body motion was investigated while comparing two initialization methods. The spinodal initialization would correspond in practice a reactive, whereas the random initialization corresponds more to the situation when the droplets and particles are formed separately and then mixed in the slag. Realistic microstructures based on actual micrographs were used for the solid particles.

The spinodal initialization was carried out for an initial supersaturation of $x_i = 0.605$, which corresponds to a volume fraction of metal of 0.219. For the random initialization, the actual initial metal fraction is: 0.202 ± 0.001; 0.202 ± 0.001; 0.205 ± 0.002 and 0.201 ± 0.001, respectively for micrographs 1 until 4, for a proposed volume fraction of 0.20. Both initialization methods were applied for a non-wetting situation ($x_S = 0.50$) and a low wetting case ($x_S = 0.60$). For the $x_S = 0.50$ case, the resulting microstructures are compared to the microstructures without the presence of rigid body motion, from our previous work [23]. For the $x_S = 0.60$ case, extra simulations without rigid body motion were conducted to be able to compare them. The microstructures for the $x_S = 0.50$ case are shown in Figure 2.

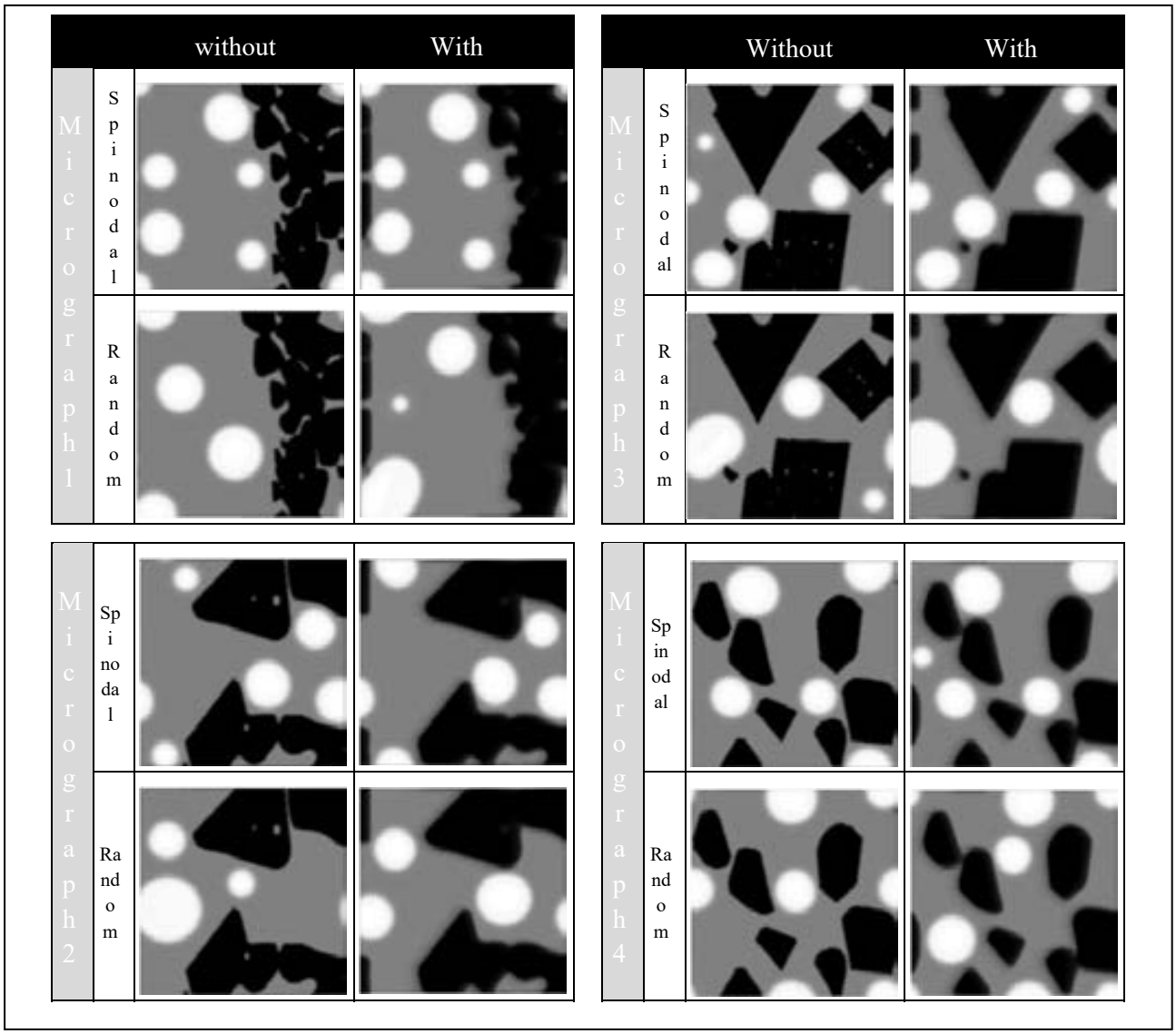

Figure 2: Comparison of the spinodal (upper row) and random (lower row) initialization methods in a non-wetting situation ($x_S = 0.50$)

The fact that the shape of the solid particles is changed, i.e. the angles and corners are softened, finds it origin in taking the kinetic coefficient for the phase field evolution larger every 100th time step, which in turn is needed to move the diffuse interface along with the bulk solid particle when rigid body motion takes place. In the no-wetting regime, the rigid body motion can be responsible for both attachment and detachment of solid particles. The area and fraction attached metal as a function of the particle fraction, which is characteristic for each micrograph, at the final 10$^{6\ th}$ simulation step, which corresponds to 100 s, are shown in Figure 3.

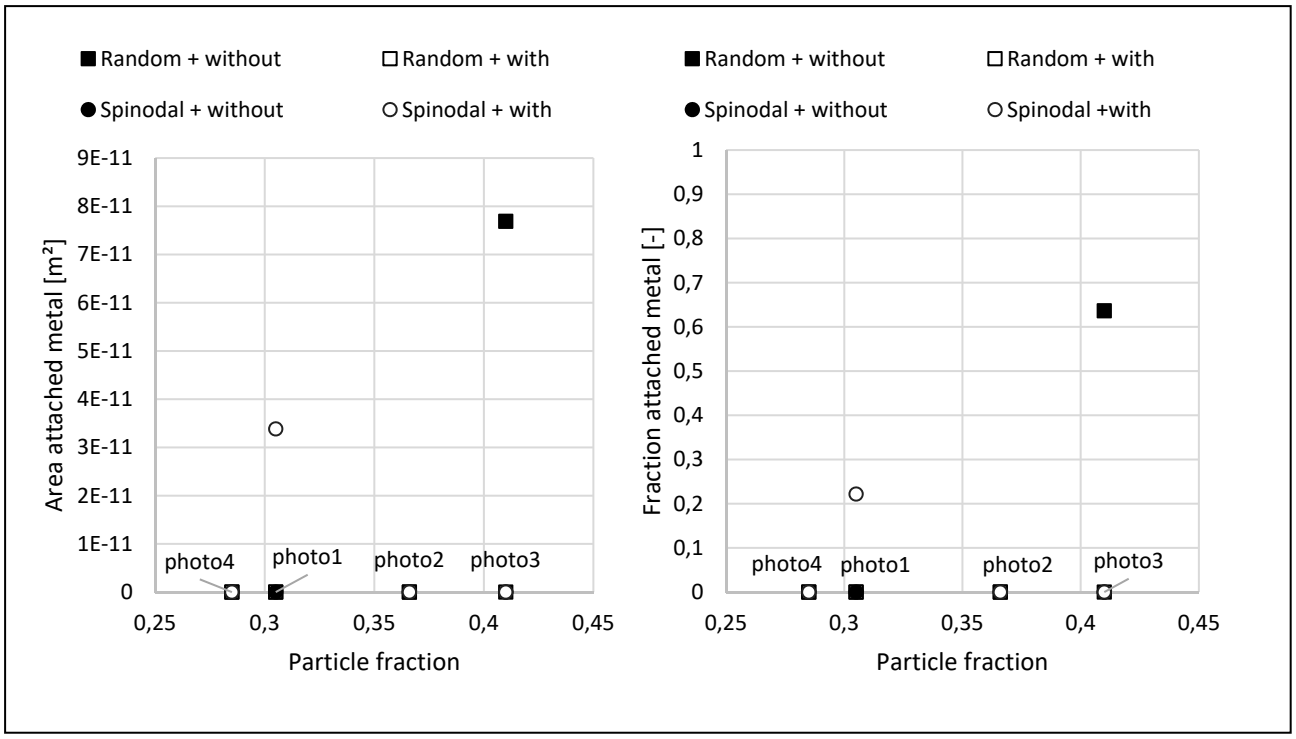

Figure 3: The area and fraction attached metal as a function of the particle fraction at the final simulation step (10^6), which corresponds to 100 s for the non-wetting case (x_S = 0.50). The particle fraction is characteristic for each micrograph, which is indicated by the label above the x-axis

In the non-wetting case, most of the metal remains non-attached. Rigid body motion can either increase the amount of attached metal, such as for the spinodal initialization for micrograph 1, or decrease it, such as for the random initialization for micrograph 3.

Whether this is also the case for the low wetting case (x_S = 0.60) is investigated qualitatively in Figure 4 and quantitatively in Figure 5.

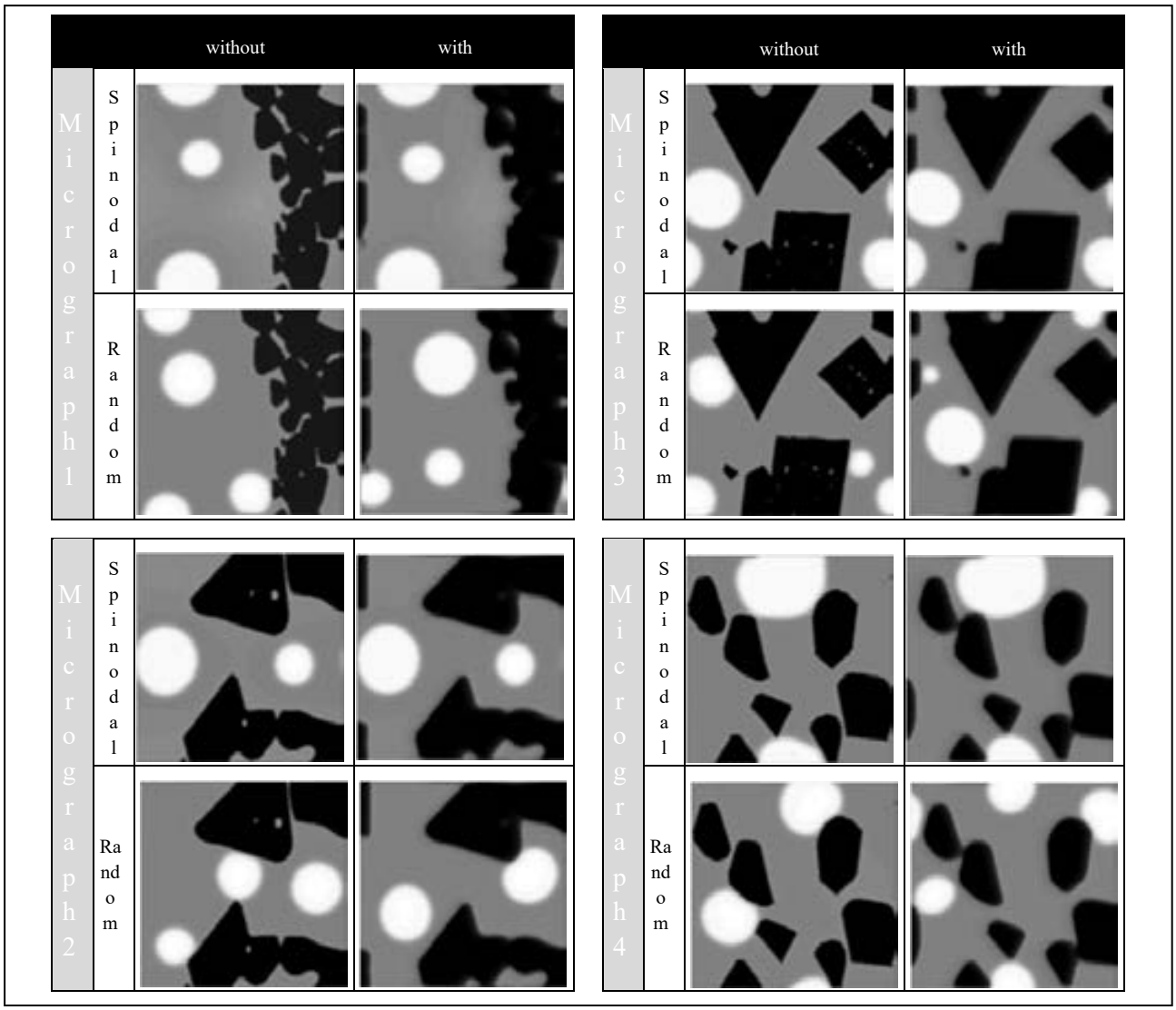

Figure 4: Comparison of the spinodal (upper row) and random (lower row) initialization methods in a low wetting situation ($x_S = 0.60$)

In the low wetting case, the rigid body motion can also cause both detachment and attachment of the metal droplets to the solid particles. But the rigid body motion seems to mainly decrease the amount of attached metal, as also illustrated in Figure 5.

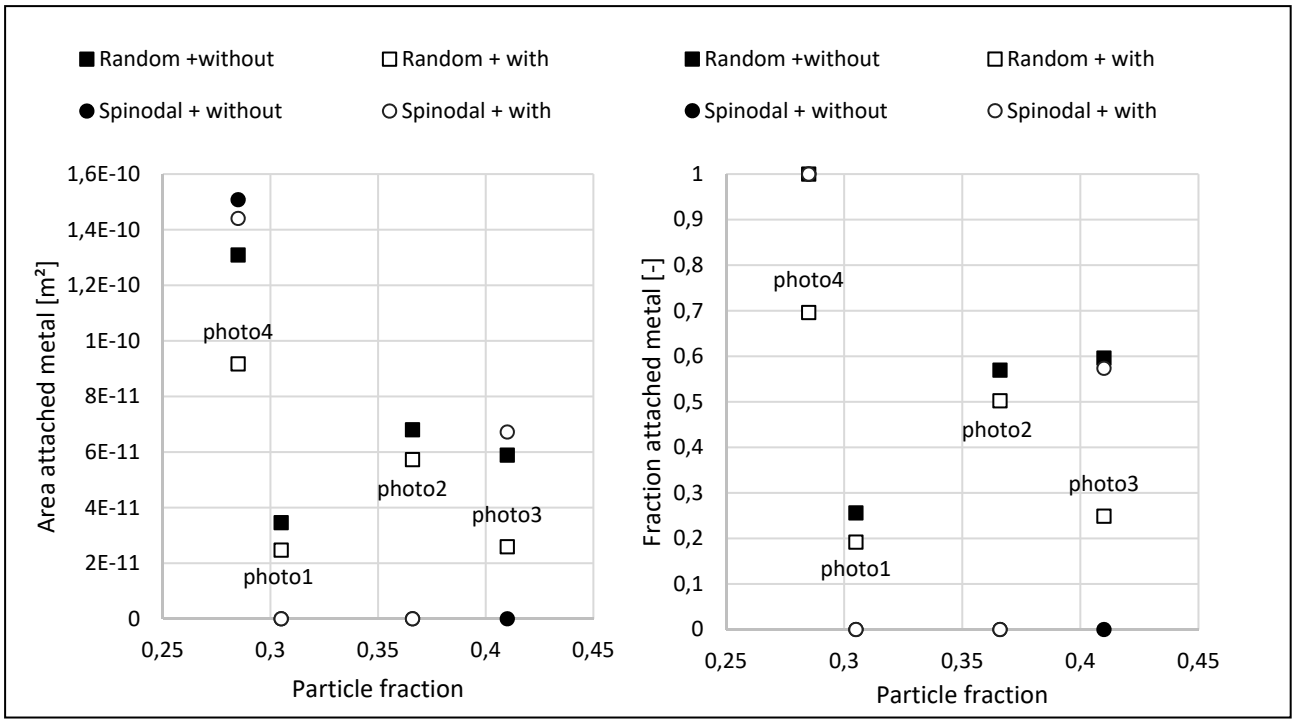

Figure 5: The area and fraction attached metal as a function of the particle fraction at the final simulation step (10^6), which corresponds to 100 s for the low wetting case (x_S = 0.60). The particle fraction is characteristic for each micrograph, which is indicated by the label above the corresponding white rectangle

In all wettability regimes, the attached metal droplets have a less spherical shape when rigid body motion is present in the system. This is clearest when the most spherical attached droplets are expected.

4 Final discussion and conclusion

This study investigated the attachment of liquid droplets to solid particles in liquid slags with a phase field model [8, 9, 23], which was extended to consider rigid body motion while considering real micrographs for the solid particles. In this model, the particles do not react with the liquid. Moreover, two initialization methods for the metal droplets were considered: by spinodal decomposition of a supersaturated liquid and a method with random positioning of the droplets. The first corresponds to a practical situation where the droplets are formed by a reaction nearby (and possibly together with) the spinel particles, whereas the latter corresponds to the situation where the droplets and particles are formed separately and then mixed randomly in the slag.

Previously, two pathways were proposed for the origin of the attachment: a reactive (corresponding to the spinodal initialization) and a non-reactive one (corresponding to the random initialization). For the reactive origin, a reaction scheme was proposed, where the spinel solids form together with the copper droplets or form around the copper droplets, depending on the local conditions of the system.

In the non-reactive pathway, it is proposed that the metal droplet and spinel particle can get attached to each other due to the large amount of mixing taking place during pyrometallurgical operations. The rigid body motion in this study is used to simulate the mixing.

Regarding the amount of attached metal, the rigid body motion did not have a lot of influence in the non-wetting case. But in the $x_S = 0.60$-case, the influence of the rigid body motion seems to increase the amount of attached metal to a small extent. The resulting micrographs can be compared to experimental observations in the FeO-SiO_2-Cu_2O-Al_2O_3 system, such as in Figure 6.

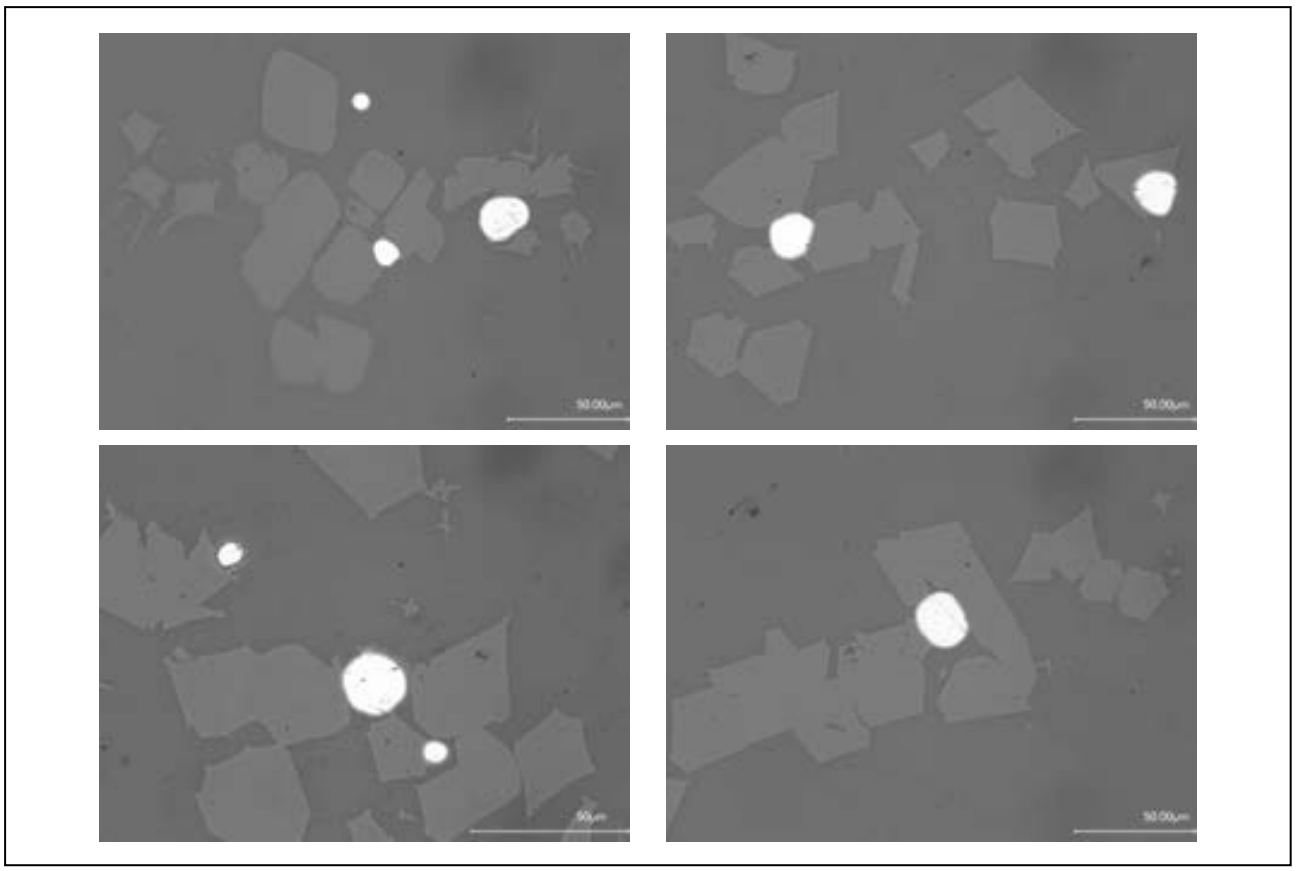

Figure 6: Experimental micrograph of Cu droplets attached to solid particles in the FeO-SiO_2-Cu_2O-Al_2O_3 system

In all wettability regimes, the attached metal droplets have a less spherical shape when rigid body motion is present in the system. This can also be observed in the experiments (Figure 6).

It can also be clearly observed than one metal droplet is surrounded by more than one solid particle in most cases. In the simulations, this behaviour is best observed for micrograh 4. Clearly, the non-wetting regime does not correspond well and the $x_S = 0.60$ case corresponds better. Moreover, the simulation in the absence or presence of rigid body motion correspond for the spinodal initialization better than the one with the random initialization.

This correspondence shows that the droplet-particle interaction could originate from a chemical interaction in which the droplet and the particle are involved, as was also confirmed by recent experi-

mental findings of De Wilde et al. [24] in a PbO-FeO-CaO-SiO_2-Cu_2O-ZnO-Al_2O_3 system: solid spinel particles grow on the edge of already existing metallic droplets. It was, however, not excluded that the spinel solids form together with the metal droplets. A mechanism for this observation was also proposed previously [24]: the spinel solids and copper droplets form together or the spinel solids can also form on an already present Cu droplet due to a simultaneous reduction of copper oxides into metallic copper and the oxidation of slag oxides into more stable spinel structures. However, the mixing or motion of the different phases with respect to each might also influence the attachment.

More simulations and experiments focussing on this hypothesis, will be executed in the future to create more clarity on this matter. Explicit implementation of a model of the formation of the solid particles within a liquid slag together with or on the side of a liquid metal droplet in a multicomponent multiphase system will allow us to simulate and study the reactive origin for the attachment in more detail.

Acknowledgments

I. Bellemans holds a PhD fellowship of the Research Foundation – Flanders (FWO).

References

[1] Sridhar R, Toguri JM, Simeonov S (1997) Copper losses and thermodynamic considerations in copper smelting. Metall Mater Trans B 28:191–200. doi: 10.1007/s11663-997-0084-5

[2] Calvo FA, Ballester A (1986) The settling of metallic lead from lead blast furnace slag. Metall Trans B 17:267–270. doi: 10.1007/BF02655073

[3] Karma A, Rappel W-J (1998) Quantitative phase-field modeling of dendritic growth in two and three dimensions. Phys Rev E 57:4323–4349. doi: 10.1103/PhysRevE.57.4323

[4] Heulens J, Blanpain B, Moelans N (2011) A phase field model for isothermal crystallization of oxide melts. Acta Mater 59:2156–2165. doi: 10.1016/j.actamat.2010.12.016

[5] Chen L-Q (2002) Phase-Field Models for Microstructure Evolution. Annu Rev Mater Res 32:113–140. doi: 10.1146/annurev.matsci.32.112001.132041

[6] Wang YU (2006) Computer modeling and simulation of solid-state sintering: A phase field approach. Acta Mater 54:953–961. doi: 10.1016/j.actamat.2005.10.032

[7] Moelans N, Blanpain B, Wollants P (2008) An introduction to phase-field modeling of microstructure evolution. Calphad 32:268–294. doi: 10.1016/j.calphad.2007.11.003

[8] Bellemans I, Moelans N, Verbeken K (2015) Phase field modelling of the attachment of metallic droplets to solid particles in liquid slags: Influence of interfacial energies and slag supersaturation. Comput Mater Sci 108, Part B:348–357. doi: 10.1016/j.commatsci.2015.03.019

[9] Bellemans I, De Wilde E, Moelans N, Verbeken K (2015) Phase field modelling of the attachment of metallic droplets to solid particles in liquid slags: Influence of particle characteristics. Acta Mater 101:172–180. doi: 10.1016/j.actamat.2015.08.074

[10] De Wilde E, Bellemans I, Campforts M, et al (2015) Wetting behaviour of Cu based alloys on spinel substrates in pyrometallurgical context. Mater Sci Technol 31:1925–1933. doi: 10.1179/1743284715Y.0000000052

[11] Allen SM, Cahn JW (1979) A microscopic theory for antiphase boundary motion and its application to antiphase domain coarsening. Acta Metall 27:1085–1095. doi: 10.1016/0001-6160(79)90196-2

[12] Osher S, Fedkiw RP (2001) Level Set Methods: An Overview and Some Recent Results. J Comput Phys 169:463–502. doi: 10.1006/jcph.2000.6636

[13] Sethian JA, Smereka P (2003) Level Set Methods for Fluid Interfaces. Annu Rev Fluid Mech 35:341–372. doi: 10.1146/annurev.fluid.35.101101.161105

[14] Cahn JW, Hilliard JE (1958) Free Energy of a Nonuniform System. I. Interfacial Free Energy. J Chem Phys 28:258. doi: doi:10.1063/1.1744102

[15] Sakai T, Ip SW, Toguri JM (1997) Interfacial phenomena in the liquid copper-calcium ferrite slag system. Metall Mater Trans B 28:401–407. doi: 10.1007/s11663-997-0105-4

[16] Sun HP, Nakashima K, Mori K (2006) Influence of slag composition on slag-iron interfacial tension. Isij Int 46:407–412. doi: 10.2355/isijinternational.46.407

[17] Moelans N (2011) A quantitative and thermodynamically consistent phase-field interpolation function for multi-phase systems. Acta Mater 59:1077–1086. doi: 10.1016/j.actamat.2010.10.038

[18] (2011) Matlab 7.12.0 (R2011a). The MathWorks Inc., Natick, MA

[19] Chen L-Q, Shen J (1998) Applications of semi-implicit Fourier-spectral method to phase field equations. Comput Phys Commun 147–158. doi: 10.1016/S0010-4655(97)00115-X

[20] De Wilde E, Bellemans I, Vervynckt S, et al (2013) Towards a methodology to study the interaction between Cu droplets and spinel particles in slags. In: Proc. EMC 2013. pp 161–174

[21] Mostafaee S, Andersson M, Jönsson P (2010) Petrographic and thermodynamic study of slags in EAF stainless steelmaking. Ironmak Steelmak 37:425–436. doi: http://dx.doi.org/10.1179/030192310X12646889256022

[22] Cahn JW (1961) On spinodal decomposition. Acta Metall 9:795–801. doi: 10.1016/0001-6160(61)90182-1

[23] Bellemans I, De Wilde E, Moelans N, Verbeken K (2016) Phase field simulation study of the attachment of metallic droplets to solid particles in liquid slags based on real slag–spinel micrographs. Comput Mater Sci 118:269–278. doi: 10.1016/j.commatsci.2016.03.022

[24] De Wilde E, Bellemans I, Zheng L, et al (online) Origin and sedimentation of Cu-droplets sticking to spinel solids in pyrometallurgical slags. Mater Sci Technol doi 10.1080/02670836.2016.1151998. doi: 10.1080/02670836.2016.1151998